NANO LETTERS

Letter

pubs.acs.org/NanoLett

Confinement in Thickness-Controlled GaAs Polytype Nanodots

Neimantas Vainorius,[†,§] Sebastian Lehmann,[†,§] Daniel Jacobsson,[†] Lars Samuelson,[†] Kimberly A. Dick,[†,‡] and Mats-Erik Pistol*[,†]

[†]Solid State Physics/The Nanometer Structure Consortium, Lund University, P.O. Box 118, SE-221 00 Lund, Sweden

[‡]also at Centre for Analysis and Synthesis, Lund University, Box 124, 221 00 Lund, Sweden

Supporting Information

ABSTRACT: Polytype nanodots are arguably the simplest nanodots than can be made, but their technological control was, up to now, challenging. We have developed a technique to produce nanowires containing exactly one polytype nanodot in GaAs with thickness control. These nanodots have been investigated by photoluminescence, which has been cross-correlated with transmission electron microscopy. We find that short (4−20 nm) zincblende GaAs segments/dots in wurtzite GaAs confine electrons and that the inverse system confines holes. By varying the thickness of the nanodots we find strong quantum confinement effects which allows us to extract the effective mass of the carriers. The holes at the top of the valence band have an effective mass of approximately 0.45 m_0 in wurtzite GaAs. The thinnest wurtzite nanodot corresponds to a twin plane in zincblende GaAs and gives efficient photoluminescence. It binds an exciton with a binding energy of roughly 50 meV, including central cell corrections.

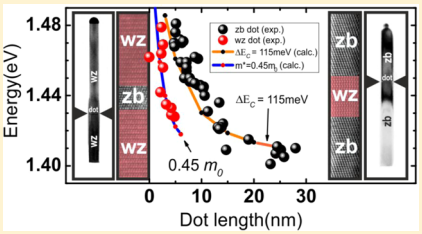

KEYWORDS: *Nanodots, nanowires, polytypism, photoluminescence*

Semiconductor nanowires, often grown from III−V semiconductors, form a very flexible system to study low dimensional physical phenomena.[1] The size and geometry of nanowires allows highly lattice mismatched materials to be grown[2,3] as heterojunctions with defect-free heterointerfaces, including highly strained nanodots. Another flexible feature of III−V nanowires is the possibility to control the crystal structure between the zincblende (zb) and wurtzite (wz) polytypes quite precisely.[4,5] The ability to perform such crystal phase engineering is so far unique for nanowires and allows new types of heterostructures to be explored, including polytype nanodots. We will call thin segments in nanowires nanodots since the lateral confinement is quite small. Nanowires containing heterostructures of zb and wz polytypes have previously been studied using transmission electron microscopy (TEM) and photoluminescence (PL),[7−13] including photon correlation studies.[14] Polytype nanodots are in some sense the simplest possible nanodots because there is no change of the constituent atoms and the strain is negligible. Even the geometrical difference is small; the difference between the zb and wz lattices only involves a change in position of 3 out of 12 atoms in the next nearest shell to a given atom.[16] We have developed a technique to produce nanowires containing exactly one polytype nanodot in GaAs with thickness control.[5,6] The tailored polytypic GaAs nanowires were seeded from Au aerosol particles and grown onto $(\overline{1}11)$ oriented epiready GaAs substrates by metal organic vapor phase epitaxy in an AIXTRON close-coupled showerhead machine at a set temperature of 580 °C, a reactor pressure of 100 mbar, and a total gas flow of 8 slm. Crystal structure control was achieved by using AsH_3 molar fractions of $\chi = 2.3 \times 10^{-5}$ and $\chi = 4.4 \times 10^{-3}$ for wz and zb growth, respectively, under otherwise identical conditions.[5] Control over the individual segment lengths in turn was achieved by adjusting the growth times. We used five different growth times to get different zincblende segment lengths (2, 4, 8, 16, and 32 s) and two different growth times for the wurtzite segments (4 and 8 s). This allows us to get good thickness control over the nanodots; however, a detailed work on tailoring polytype heterostructures will be published separately.

Using this technique we have performed a study of single zb-GaAs nanodots in wz-GaAs nanowires as well as of single wz-GaAs nanodots in zb-GaAs nanowires as a function of dot thickness. We attained the limit of the shortest possible wz-dot. Such a wz-dot can also be seen as a twin plane in zb-GaAs and we find that it binds an exciton with a binding energy of about 50 meV. This is the total binding energy that includes possible single-particle binding energies. Neither single polytype nanodots nor single twin planes have previously been fabricated in III−V semiconductors.

Each nanowire in this study was measured both in PL and by TEM, which gives very accurate structural input for theoretical calculations of the confinement. A subset of the PL/TEM-investigated nanowires were also investigated by scanning electron microscopy (SEM). The confinement effects were calculated using a single-band effective mass model. For the PL and TEM measurements, we removed the nanowires from the growth substrate by ultrasonication in methanol and transferred

Received: January 21, 2015
Revised: March 3, 2015
Published: March 11, 2015

DOI: 10.1021/acs.nanolett.5b00253
Nano Lett. 2015, 15, 2652−2656

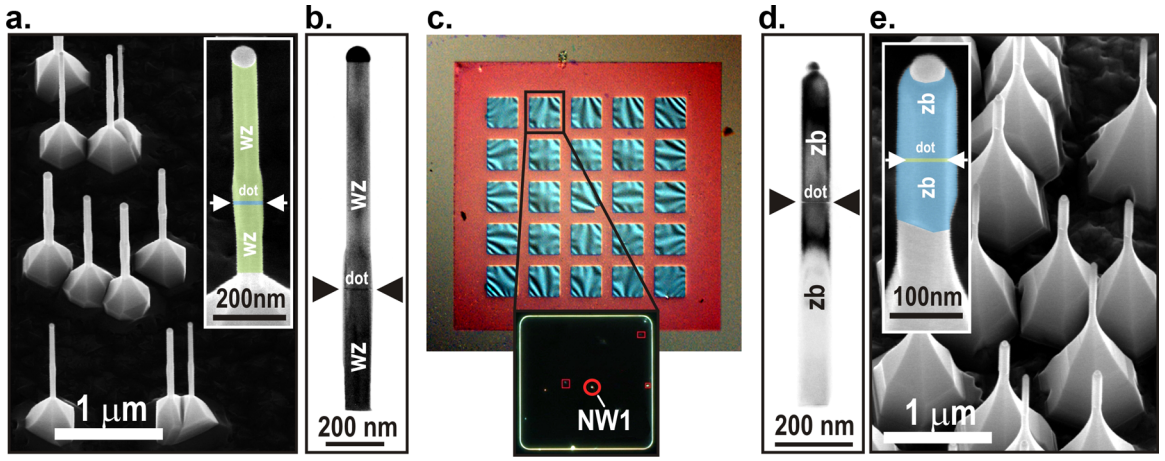

Figure 1. SEM images, 30-tilted view, with higher magnification insets of GaAs nanowires with a zincblende dot embedded in otherwise wurtzite material (a) and nanowires with a wurtzite dot embedded in otherwise zincblende material (e). The insets are additionally false-colored (green wz, blue zb) as a guide to the eye. Bright field TEM images of single nanowires identical to the ones given in (a) and (e) are presented in (b) for the zb-dot and (d) for the wz-dot, where the spatial position of the dots in the nanowires are visible by contrast differences in the TEM images and are additionally highlighted. High-resolution TEM and selected area diffraction in the TEM was used to confirm the crystal structure as it is labeled in the figures. An optical microscope image of a TEM grid with 25 electron-transparent SiN_x sections is exemplarily shown in (c). Higher magnification inset of one section at the bottom is given in addition where nanowires can be recognized as higher contrast spots to schematically describe the approach used for analyzing identical nanowires in PL and TEM.

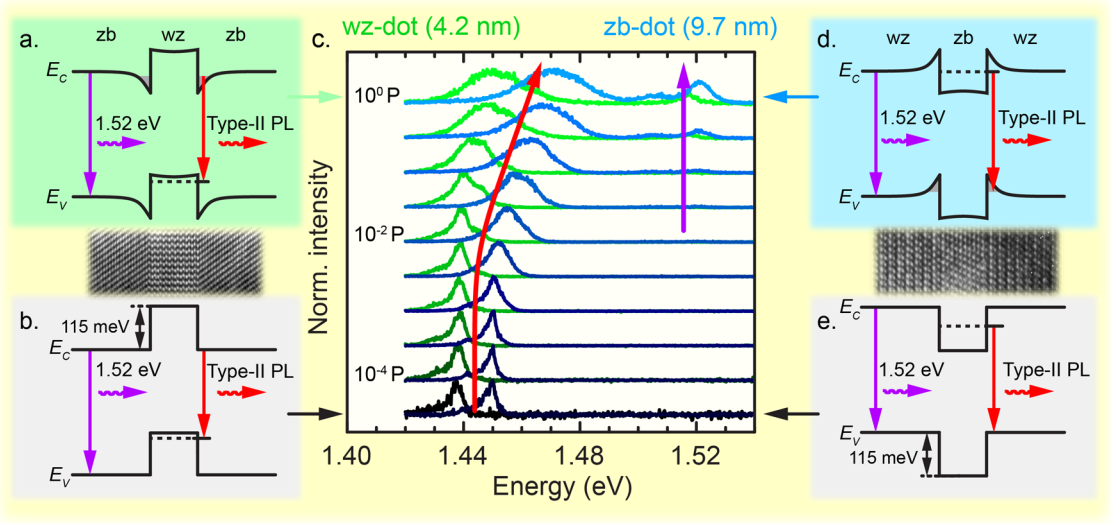

Figure 2. Band diagram of wz-GaAs nanodots (a, b) and zb-GaAs nanodots (d, e) at low (b, e) and high (a, d) excitation power density, along with representative HRTEM-images. (c) PL spectra of both type of dots, as a function of excitation power density. We attribute the blue-shifting peak to type-II recombination of electrons (holes) in the nanodot with holes (electrons) in the wz-GaAs (zb-GaAs) surrounding. The green traces correspond to a wz-dot and the blue traces to a zb-dot.

them onto TEM grids. Using an optical microscope the transferred nanowires were carefully mapped out, so that the same single nanowires could be identified and studied by both PL and TEM. The PL was performed at 7 K using an optical microscope to collect the light. The excitation source was a frequency doubled yttrium−aluminum−garnet laser and a cooled charge coupled device camera was used as a detector. We always performed the optical measurements before the TEM-investigations. All our data (TEM images and PL spectra of 50 nanowires) are given in the Supporting Information.[18]

In Figure 1, we show overview SEM images as well as bright field TEM images of our wires. There is substantial growth at the base of the wires, which is not present, however, in the transferred wires. The figure also shows an optical image of a TEM grid on which nanowires were deposited illustrating the experimental method.

In Figure 2 we present PL data of single nanodots at different excitation power densities. The figure also contains exemplary high resolution (HR)TEM-images of zb and wz dots and schematics of the band-diagrams at low and high excitation power densities. The HRTEM shows that the interfaces are atomically sharp and contain no twin planes either in the dots or in the vicinity of the dots. However, for many nanowires, we do observe twin defects in zb dots and stacking defects in wz dots in otherwise stacking defect free host materials. These defects do not seem to affect the PL in any cleancut way. We observe several emission peaks in the spectra. The high energy peaks, having energies around 1.51−1.52 eV are due to GaAs

DOI: 10.1021/acs.nanolett.5b00253
Nano Lett. 2015, 15, 2652−2656

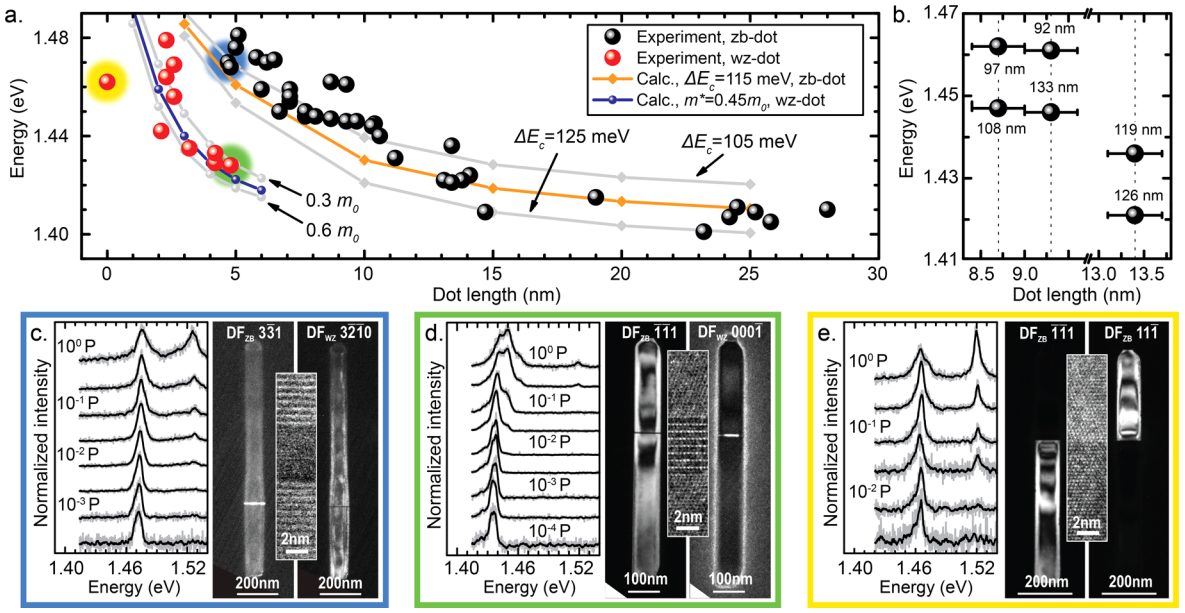

Figure 3. (a) Transition energy of wurtzite and zincblende dots as a function of dot length along with calculated transition energies. The calculations were done using different effective masses for the holes as well as using different band offsets when calculating the electron confinement. (b) Transition energies of six different dots with the diameters of the nanowires indicated. The transition energies are higher for dots in smaller diameter wires, despite having the same length. We assume an uncertainty in dot length of one bilayer spacing along the ⟨111⟩/⟨0001⟩-type direction (0.3 nm) at each interface, which is very conservative. Bottom panels show dark field (DF) and HRTEM-images of three different dots using wurtzite and zincblende specific diffraction spots, respectively, for imaging as indicated in (c, d, e). The bottom panels also show their spectra as a function of excitation power density. Energy diagrams of (c) a 4.8 nm zb-dot, (d) a 4.8 nm wz-dot, and (e) a twin plane. Gray traces are raw data, black traces are smoothed. The color of the frames corresponds to the color of the highlighted data points in (a).

barrier emission. For zb-GaAs barriers this emission is due to the recombination of free excitions, and we suspect the same for wz-GaAs barriers. Please note that the barrier emission energy is very similar for wz-GaAs and zb-GaAs. This is in agreement with recent reports that the two polytypes have very similar bandgaps.[13,19] The energy of these peaks do not depend on excitation power density unless it is very high, where laser heating takes place and the peak redshifts. The low energy peaks blue shift with increasing excitation power. We do not always observe a blue-shifting peak. The nanowires that do not show the blue-shifting peak were in the zb-dot series and always had a blister-like structure around the nanodot, as observed by TEM and scanning electron microscopy (see ref 5 for structural characterization of this). They also have very weak PL in general. Nanowires without this blister-like structure always show a shifting peak and give much stronger PL. A blue-shifting peak is a well-known behavior of type II band alignment systems and has been observed in other material systems, such as GaSb/GaAs nanodots,[20] as well as in our previous studies of single wz-GaAs and zb-GaAs heterojunctions.[13] In Figure 2, we give schematics illustrating the bandstructure at low and high excitation power density. Using zb-dots as an example, we have electrons confined in the zb nanodot and the holes are confined in the wz-barrier, giving spatially indirect transitions. For increasing excitation power density, we get band bending and state filling both in the zb nanodot and in the triangular wz quantum well. This will cause a blue shift of the emission because the dominant recombination is between electrons and holes at the quasi-Fermi levels where the wave function overlap is highest. The transition energy at sufficiently low excitation power density allows the quantum confinement to be measured. When the nanodot thickness becomes smaller, we need a higher excitation power density to shift the peak. In fact, for the thinnest nanodots, we have difficulty observing any shift at all before heating the nanowire. Our explanation is that the overlap between the wave functions of electrons and holes becomes larger for the thinner nanodots. This results in an increased recombination rate of carriers, meaning that a higher excitation power density is required to introduce enough charge carriers to cause detectable band-bending and state-filling effects.

In Figure 3, we show the transition energies as a function of dot length (i.e., segment length along the nanowire growth axis) for both zincblende and wurtzite dots, along with calculated transition energies. The type II emission often consists of several overlapping peaks, possibly due to excited states in the triangular quantum well in the barrier. We extracted the lowest energy transition by fitting the emission peak with two or three gaussians. Each data point correspond to a nanowire that has been measured both in PL and imaged by HRTEM, giving error bars that are smaller than the data points. We find that there is considerable scatter in the transition energies, which we will discuss later. We also find that for a given length of the dots we have a lower transition energy for wz-GaAs dots than for zb-GaAs dots. In the figure, we show PL spectra from a wz-GaAs dot and a zb-GaAs dot along with TEM-images of the same dots. The length of both dots is 4.8 nm, but the emission energy differs by 40 meV. This is due to a higher effective mass of the confined charge carriers (holes) in wz-GaAs dots.

The calculations were performed using a single-band one-dimensional effective mass model assuming equal effective masses in the barrier and in the dots. A single-band model is not expected to be very accurate for the valence band. However, it is more motivated for wurtzite semiconductors than for zincblende semiconductors because the top of the

DOI: 10.1021/acs.nanolett.5b00253
Nano Lett. 2015, 15, 2652−2656

valence band is then not orbitally degenerate in contrast to the situation in zincblende semiconductors.[16] Using an effective mass of 0.067 m_0 for electrons, 0.45 m_0 for holes and a valence band offset of 115 meV, with zb-GaAs having the lowest energy, we get the computed data points in the figure. In order to get a handle of the uncertainties, we calculated the confinement for the holes using three different hole masses, 0.3 m_0, 0.45 m_0, 0.6 m_0, while keeping the valence band offset constant. For the electron confinement, we kept the effective mass constant but varied the valence band offset, 0.105, 0.115, and 0.125 eV. The agreement with the experiment is good, and we confirm that zb-GaAs confines electrons and wz-GaAs confines holes, as has been theoretically predicted.[15] The valence band offset that we determine is in good agreement with theoretical predictions and previous experiments.[7,9,11−13,15] The hole effective mass that we determine in wz-GaAs is the same as for the heavy hole in zb-GaAs,[17] but we note that the uncertainty in our determination is quite high. We used the GaAs electron mass given in ref 17, which should be appropriate for the zb-GaAs dots.

The thinnest wz-GaAs dot that we could produce can also be seen as a twin plane in zb-GaAs. So far, we have measured only one twin plane, due to a low yield of fabrication. We are trying to improve the yield. Figure 3 shows DF and HRTEM-images of a twin plane and the corresponding PL spectra from the imaged wire. The PL has an energy of 1.46 eV. A twin plane can be seen as an isoelectronic[21] defect, which according to our experiment binds excitons with a binding energy of 50 meV. The emission energy for the twin plane is lower than the emission energy of some thicker nanodots, which indicates that the simple model we use is not so adequate to describle very thin nanodots. We speculate that the twin plane initially binds a hole that subsequently electrostatically binds an electron; that is, the twin plane may behave analogously to an isoelectronic donor.[22] Because the twin plane is planar, we should at higher excitation densities have a sheet of polarized excitons, positively charged in the center and negatively charged at the surface. Polarized excitons in 2D have been predicted to have a rich phase diagram,[23,24] and we hope that twin planes in zb-GaAs can be used to study these phases, which include the exotic Wigner supersolid.

We have found that smaller diameter nanowires usually contain dots having higher transition energies than thicker wires, despite the dot length being exactly the same. This is illustrated in Figure 3b, where we have zoomed in on some data points from Figure 3a. The wire thicknesses are given in the figure. Calculations show that the scatter in transition energies is not due to lateral confinement. Instead, it appears that the surface influences the transition energies. There are many possible reasons, such as bandbending at the surface, surface charges, and so forth, and it is premature to give specific conclusions at this stage. It should be noted that the nanowires we have investigated are uncapped and not covered with an AlGaAs shell. We have found that an AlGaAs shell introduces extra complications such as anisotropic growth and composition variations when grown on the different polytypes. These effects lie outside the scope of the presented study and will be the focus of a future work.

The possibility of making single polytype dots in GaAs opens many new areas for future research, and we will mention a few. An obvious generalization of the present work is to investigate polytype superlattices both optically and electrically. Polytype dots are very simple, which allows atomistic bandstructure theories to be tested in a new way. The transition between the twin plane and longer dots should be carefully investigated with respect to excitonic effects. Precisely how the surface and a possible shell affects the transition energies is important to clarify.

■ ASSOCIATED CONTENT

Supporting Information

Experimental spectra and TEM images for all investigated nanowires as well as the growth details. This material is available free of charge via the Internet at http://pubs.acs.org/.

■ AUTHOR INFORMATION

Corresponding Author

*E-mail: Mats-Erik.Pistol@ftf.lth.se.

Author Contributions

§These authors contributed equally to this work.

Notes

The authors declare no competing financial interest.

■ ACKNOWLEDGMENTS

This work was performed within the nanometer structure consortium in Lund (nmC@LU) and supported by the Swedish Foundation for Strategic Research (SSF), nmC@LU, the Knut and Alice Wallenberg Foundation, the Swedish Research Council (VR) and by the EU program NWs4Light under Grant No. 280773. S.L. gratefully acknowledges the support by a fellowship within the Postdoc-Programme of the German Academic Exchange Service (DAAD).

■ REFERENCES

(1) Duan, X.; Huang, Y.; Cui, Y.; Wang, J.; Lieber, C. M. *Nature* **2001**, *409* (6816), 66−69.

(2) Björk, M. T.; Ohlsson, B. J.; Sass, T.; Persson, A. I.; Thelander, C.; Magnusson, M. H.; Deppert, K.; Wallenberg, L. R.; Lars Samuelson, L. *Nano Lett.* **2002**, *2*, 87.

(3) Glas, F. *Phys. Rev. B* **2006**, *74*, 121302.

(4) Caroff, P.; Bolinsson, J.; Johansson, J. *IEEE J. Sel. Top. Quantum Electron.* **2010**, 18.

(5) Lehmann, S.; Jacobsson, D.; Deppert, K.; Dick, K. A. *Nano Res.* **2012**, *5*, 470.

(6) Bao, J.; Bell, D. C.; Capasso, F.; Wagner, J. B.; Mårtensson, T.; Trägårdh, J.; Samuelson, L. *Nano Lett.* **2008**, *8*, 836.

(7) Kurananda, P.; Montazeri, M.; Gass, R.; Smith, L. M.; Jackson, H. E.; Yarrison-Rice, J.; Paiman, S.; et al. *Nano Lett.* **2009**, *9*, 648.

(8) Spirkoska, D.; Arbiol, J.; Gustafsson, A.; Conesa-Boj, S.; Glas, F.; Zardo, I.; Heigoldt, M.; Gass, M. H.; Bleloch, A. L.; Estrade, S.; Kaniber, M.; Rossler, J.; Peiro, F.; Morante, J. R.; Abstreiter, G.; Samuelson, L.; Fontcuberta i Morral, A. *Phys. Rev. B* **2009**, *80*, 245325.

(9) Heiss, M.; Conesa-Boj, S.; Ren, J.; Tseng, H.-H.; Gali, A.; Rudolph, A.; Uccelli, E.; et al. *Phys. Rev.* **2011**, *B83*, 045303.

(10) Ahtapodov, L.; Todorovic, J.; Olk, P.; Mjåland, T.; Slåttnes, P.; Dheeraj, D. L.; van Helvoort, A. T. J.; Fimland, B.-O.; Weman, H. *Nano Lett.* **2012**, *12*, 6090.

(11) Belabbes, A.; Panse, C.; Furthmuller, J.; Bechstedt, F. *Phys. Rev.* **2012**, *B86*, 075208.

(12) Jahn, U.; Lahnemann, J.; Pfuller, C.; Brandt, O.; Breuer, S.; Jenichen, B.; Ramsteiner, M.; Geelhaar, L.; Riechert, H. *Phys. Rev. B* **2012**, *85*, 045323.

(13) Vainorius, N.; Jacobsson, D.; Lehmann, S.; Gustafsson, A.; Dick, K. A.; Samuelson, L.; Pistol, M.-E. *Phys. Rev. B* **2014**, *89*, 165423.

(14) Akopian, N.; Patriarche, G.; Liu, L.; Harmand, J.-C.; Zwiller, V. *Nano Lett.* **2010**, 10.

(15) Murayama, M.; Nakayama, T. *Phys. Rev.* **1994**, *B49*, 4710.

(16) De, A.; Pryor, C. *Phys. Rev. B* **2010**, *81*, 155210.

DOI: 10.1021/acs.nanolett.5b00253
Nano Lett. 2015, 15, 2652−2656

(17) Vurgaftman, I.; Meyer, J. R.; Ram-Mohan, L. R. *J. Appl. Phys.* **2001**, *89*, 5815.
(18) See Supporting Information.
(19) Ketterer, B.; Heiss, M.; Uccelli, E.; Arbiol, J.; Fontcuberta i Morral, A. *ACS Nano* **2011**, *5*, 7585.
(20) Hatami, F.; Ledentsov, N. N.; Grundmann, M.; Bhrer, J.; Heinrichsdorff, F.; et al. *Appl. Phys. Lett.* **1995**, *67*, 656.
(21) Dean, P. J. *J. Lumin.* **1973**, *7*, 51.
(22) Hopfield, J. J.; Thomas, D. G.; Lynch, R. T. *Phys. Rev. Lett.* **1966**, *17*, 312.
(23) Hartmann, P.; Donko, Z.; Kalman, G. *Europhys. Lett.* **2005**, *72*, 396.
(24) Joglekar, Y. N.; Balatsky, A. V.; das Sarma, S. *Phys. Rev. B* **2006**, *74*, 233302.

DOI: 10.1021/acs.nanolett.5b00253
Nano Lett. 2015, 15, 2652−2656